JAM
Japanese Acupuncture and Moxibustion

Original Research

Increase of molecular chaperone αB-crystallin expression in the rat soleus muscle induced by moxa needle stimulation

YAJIMA Michiko, SUMIYA Eiji, KAWAKITA Kenji, YANO Tadashi

Course of Acupuncture and Moxibustion, Graduate School of Acupuncture and Moxibustion, Meiji University of Integrative Medicine

Abstract

[Background] The purpose of this study is to investigate whether the expression of αB-crystallin in slow soleus muscles is affected by thermal stimulation in moxa needle therapy. αB-crystallin is known to be abundant in slow muscles and to maintain and improve the function of slow antigravity muscles. Moxa needle used to be performed with silver needles, which have high thermal conductivity, but is currently performed with stainless steel needles, which have low thermal conductivity. Therefore, we performed thermal stimulation with both types of moxa needles and compared their effects.

[Methods] We carried out experiments in two steps: Experiments A and B. Rats were divided into moxa needle combustion groups using silver (CSV group) and stainless steel (CSS group) needles, non-combustion groups using silver (NSV group) and stainless steel (NSS group) needles, and a control group with no needle insertion (CON group). The moxa balls in the CSV and CSS groups were burned three times intermittently. In Experiment A, skin surface and deep tissue temperatures were measured for 50 minutes. Experiment B was performed in a similar manner without deep tissue temperature measurements. At 3 hours after stimulation, the rats were euthanized. Their soleus and extensor digitorum longus (EDL) muscles were then removed to examine the expression of αB-crystallin and the relationship with deep temperature obtained from Experiment A.

[Results] In Experiment A, higher skin surface and deep temperatures were observed in the CSV than in the CSS group. In Experiment B, the skin surface temperatures in the CSV and CSS groups followed similar courses to those in Experiment A. In addition, αB-crystallin expression in soleus after correction for glyceraldehyde 3- phosphate dehydrogenase (GAPDH) expression, relative to the CON group (100), was 299.29 in the CSV, 160.62 in the CSS, 121.51 in the NSV, and 67.52 in the NSS group, indicating that αB-crystallin expression was significantly higher in the CSV than in the CON group ($P < 0.01$). No significant differences were found in the EDL.

[Conclusion] The results of this study suggest that a deep temperature increase of 4–5 °C for about 3 minutes is needed to increase αB-crystallin expression. Therefore, in moxa needle stimulation to the posterior surface of the lower leg, the use of silver needles with high thermal conductivity could increase the deep temperature and expression of αB-crystallin in soleus muscles.

Key words: *molecular chaperone, heat shock protein, αB-crystallin, moxa needle, soleus*

I. Introduction

Molecular chaperones are cellular proteins whose function is to ensure that the folding of certain other polypeptide chains and their assembly into oligomeric structures occur correctly, and they do not form part of the final structure[1]. Molecular chaperones promote efficient protein folding and prevent or reverse protein aggregation[2]. And chaperones and proteases consist of "protein quality control" network, and repair protein aggregation[2].

As the target of this research, we selected αB-crystallin, a small (22 kDa) molecular chaperone. It is presumed that αB-crystallin protects proteins from proteolysis by refolding damaged proteins[3]. Alpha B-crystallin is one of the major lens structural proteins in the vertebrate eye[3], but it also exists in a variety of tissues, including the heart, brain, kidney, and skeletal muscle[4]. Among the skeletal

Corresponding author: Yajima Michiko, Course of Acupuncture and Moxibustion, Graduate School of Acupuncture and Moxibustion, Meiji University of Integrative Medicine, Hiyoshicho, Nantan City, Kyoto 629-0392, JAPAN

muscles, αB-crystallin is known to be abundant in slow muscles[5]. Under microgravity and during atrophy of slow antigravity muscles, this chaperone tends to decrease specifically[6–8]. Alpha B-crystallin exists to maintain and improve the function of slow antigravity muscles, and its increased expression stabilizes cell function[9,10]. The expression of αB-crystallin is strongly induced by high temperatures and is effective in suppressing protein thermal aggregation[2,3].

In this study, to provide heat stimulation, we used moxa needle. The moxa needle therapy (in Japanese *kyutoshin*; "needle with moxa on the head") was spread by Tomooki Sasagawa at the end of the nineteenth century in Japan[11–13]. In moxa needle therapy, acupuncture needles are inserted into the body, and then a small moxa ball is attached to the handle of the needle and burned with the aim of obtaining the synergistic effects of acupuncture and moxibustion.

Currently, stainless steel needles are commonly used, but in the early days of moxa needle therapy, silver needles were used, and as silver has high thermal conductivity, it was possible to provide stimulation by not only radiative, but also conductive heat transfer. Therefore, moxa needle therapy was once also called "Conductive Heat Transfer Needle Therapy (*dennetsu hari ryohou*)"[13]. It is presumed that silver needles allow more heat to reach the deep tissues than do stainless steel needles, so "Conductive Heat Transfer Needle Therapy" may have an effect on increasing molecular chaperones as heat shock proteins in muscle.

To our knowledge, no studies have been conducted on the effect of moxa needle therapy on the expression of molecular chaperones. Previous studies have reported increases in molecular chaperones after soaking in hot water or placing in a hot chamber as thermal stimulation for extended periods of time[14–19]. However, if a method can be devised that is more effective and easier to perform by not requiring lengthy exposure to high temperatures, it could become more clinically applicable. It is speculated that moxa needle with silver needles, which can be expected to raise the deep tissue temperature, could provide a stressful of temperature rise in a short period of time.

Given this background, the purpose of this study is to investigate whether thermal stimulation in moxa needle therapy affects the expression of αB-crystallin, a small molecular chaperone, in slow soleus muscles and to compare the effectiveness of with silver and stainless steel needles in moxa needle for delivering thermal stimulation to deep tissues.

In order to produce a greater stressor, the burning of the moxa ball was performed three times repetitively, and the stressor was also generated by repeating the rise and fall of the temperature. Repeated burning of moxa several times has also been a clinical technique[11,12].

If moxa needle affects the expression of αB-crystallin, it could lead to the development of a new method for maintaining slow muscles, and thereby a new concept of acupuncture and moxibustion for frailty and sarcopenia in older adults in a super-aging society.

II. Methods

1. Heat stress production and temperature measurements

We measured the temperature change of the needle body of moxa needles with silver and stainless steel needles, and examined the difference in heat conduction between the two. Based on that, we carried out the experiment in rats in two steps: Experiments A and B.

All rats were housed in cages in groups of two to three in a room with controlled environmental conditions (ambient temperature 24°C ± 2°C, humidity 50% ± 10%, 12-hour light/12-hour dark cycle) and were allowed ad libitum access to food and water.

In total, 60 male Wistar rats, 9 weeks old (Japan SLC, Inc., Shizuoka, Japan), were randomly divided into 10 groups, with the following five groups each set for both Experiments A and B (n = 6/group): moxa needle, i.e., combustion groups using silver needles (CSV) and stainless steel needles (CSS), non-combustion groups using silver needles (NSV) and stainless steel needles (NSS), and a control group with no needle insertion (CON).

The temperature in the room where the data was measured was 26 ± 0.5°C and the humidity ranged from 25% to 40%.

This study was approved by the Animal Care and Use Committee of Meiji University of Integrative Medicine. (Approval No. 2021006, 2021008)

(1) Pre-measurement—needle body temperature

Silver or stainless steel needles with a length of 50 mm and a diameter of 0.27 mm (Maeda Toyokichi Shouten Co. Ltd., Tokyo, Japan) are inserted 13 mm perpendicular to polystyrene foam surface, the distance from the moxa ball to the surface was 38 mm, and the needle body temperature just above the foam surface were measured every second for 50 minutes (n = 6).

The moxa needle procedure was that a 0.9 g ± 0.005 g moxa ball with a diameter of 20 mm was attached to the handle of the needle, the measurements were started, and then the moxa ball was ignited 10 minutes later. The ignition point was the top of the moxa ball. After 7 minutes of ignition, the needle was left inserting and the burned moxa ball was removed and replaced with another ball. The next ignition was 8 minutes and 30 seconds after the previous ignition, and this procedure was performed three times in total. After the third burning, the needle were not removed and the measurement continued until 50 minutes after the start of the measurement.

(2) Experiment A: temperature measurements

Silver has the highest thermal conductivity among all

metals, whereas that for stainless steel is extremely low. In Experiment A, we researched the degree of difference in deep tissue temperature changes of the soleus muscle region when moxa needle was performed using needles made of either silver or stainless steel, by inserting a needle probe for deep tissue temperature measurements.

In Experiment A, 30 male Wistar rats, 9 weeks old, the mean (SD: standard deviation) weight 304.7 (14.6) g, were divided into five groups (n = 6/group): CSV, CSS, NSV, NSS, and CON, and were anesthetized with a triple anesthetic (medetomidine [0.15 mg/0.15 ml/kg], midazolam [2 mg/0.4 ml/kg], butorphanol [2.5 mg/0.5 ml/kg]; dose 0.25 ml/100 g).

For the rats in the CSV and CSS, combustion groups of moxa needle, the lower legs were shaved, and moxa needle was performed to the posterior aspect of the right lower leg (midpoint between the knee joint and the ankle joint on the posterior midline of the lower leg). And a needle probe for measuring the temperature of deep tissue (MT-26/4HT, Muromachi Kikai Co. Ltd., Tokyo, Japan) was inserted 16 mm at a 38° ± 5° angle to the needle from a position 10 mm outside the needle insertion point on the skin surface. And another probe for measuring the skin surface temperature was attached at 2 mm distal from the needle insertion point along the posterior midline of the lower leg.

Regarding moxa needle, silver or stainless steel needles (length 50 mm, diameter 0.27 mm) were inserted 13 mm ± 1 mm perpendicular to the skin surface. The acupuncture needle passed through gastrocnemius muscle and reached soleus muscle, and the apex of the needle was just past the side of the fibula, and this point was confirmed in a preliminary experiment by making an incision where the needle would pass, and the penetration depth and angle of the acupuncture needle and probe needle were determined. And a 0.9 g ± 0.005 g moxa ball (diameter 20 mm) was attached to the handle of the needle and left for 10 minutes. After that, the measurements were started and the moxa ball was ignited 10 minutes later. Ignition point and intervals were the same as in the pre-experiment, and three combustions were performed.

From the beginning, the deep tissue temperature at the tip of the acupuncture needle and the skin surface temperature near the needle insertion point were measured every second for 50 minutes, and then the needle was removed.

For the non-combustion groups (NSV and NSS), silver or stainless steel needles were inserted and a moxa ball was attached, and the same period of time as in the moxa needle groups passed without ignition. The same period of time also passed in the CON group, but without the insertion of acupuncture needles. The time courses of the skin surface and deep tissue temperatures were compared and examined by the mean value for each group.

In all groups, after the measurements, the rats were euthanized with an overdose of pentobarbital (200 mg/kg, intraperitoneal [i.p.] injection. Pentobarbital Sodium Salt, NACALAI TESQUE, INC., Kyoto, Japan).

(3) Experiment B: αB-crystallin protein expression measurements

In Experiment B, 30 male Wistar rats, 9 weeks old, the mean (SD) weight 306.6 (7.50) g, were used. In Experiment B, the usual moxa needle stimulation was performed without insertion of a thermal probe; all other procedures were the same as those in Experiment A. Next, we compared the intensity of expression of αB-crystallin in the soleus (red slow muscle) and the extensor digitorum longus (EDL, white fast muscle), and examined the relationship with deep tissue temperature measured in Experiment A.

Since the expression of αB-crystallin was greater 3 hours after the end of stimulation in the pre-study (data not shown), excision of muscle was performed 3 hours after the end of stimulation in this study. At 3 hours after the end of measurement, the rats were euthanized with an overdose of pentobarbital (200 mg/kg, i.p.), and their entire soleus and EDL, respectively, and eyeballs (positive control) were removed, weighed, quickly frozen by liquid nitrogen, and stored at −80°C.

2. Muscle preparation, SDS-PAGE, Western blotting and chemiluminescence detection

Approximately 0.05 g soleus and 0.06 g EDL (each half of the extracted) were frozen in liquid nitrogen and then pulverized. The powder was homogenized in Hepes buffer (25 mM Hepes, pH 7.4, 2 mM EDTA, 250 mM sucrose, 0.1% Triton, one tablet of protease inhibitor/50 ml). The homogenate was centrifuged at 16,000×g for 20 minutes at 4°C, samples were prepared from supernatants. Treated samples were subjected to sodium dodecyl sulfate (SDS)-polyacrylamide gel electrophoresis (PAGE), and we used a home-made gel. Protein contents were determined using the Bradford Protein Assay. Each lane was loaded with a protein sample from a different rat, 10 μg proteins were applied per gel lane. The gel was run for 80 minutes at 130 V.

Then transferred to polyvinylidene fluoride (PVDF) membranes at 0.8 mA/cm^2 for 45 minutes by a semi-dry system. As αB-crystallin is a small molecular chaperone, a transfer membrane with a pore size of 0.2 μm was used. After blocking with 0.1% skim milk powder for 1 hour at room temperature, the membranes were incubated with anti-αB-crystallin antibody (15808-1-AP, 1000-fold dilution, Proteintech Group, Inc, Tokyo, Japan) for 1 hour at room temperature to conjugate. After rinsing with a buffer containing 0.1% Tween20, the membranes were incubated with anti-rabbit IgG-HRP (cat. no. 7074, 5000-fold dilution, Cell Signaling Technology, Inc, Tokyo, Japan) at room temperature for 1 hour to conjugate. The bands were detected by chemiluminescence (Immobilon Crescendo Western HRP substrate, Merck KGaA, Darmstadt, Germany), imaged on X-ray film (BioMax Light-1film, Carestream Health, Inc., Tokyo, Japan),

digitized with a scanner (DocuCentre-VII C7788, FUJIFILM Corporation, Tokyo, Japan), quantified with the image analysis software Image J, and corrected by the expression level of glyceraldehyde 3-phosphate dehydrogenase (GAPDH) as internal control with anti-GAPDH (M171-7 Anti-GAPDH mAb-HRP-DirecT, 10000-fold dilution, MEDICAL & BIOLOGICAL LABORATORIES CO., LTD., Tokyo, Japan). The levels of αB-crystallin are shown in arbitrary units (a.u.) divided by those of GAPDH, and the control group was set as 100.

3. Statistics

All statistical analyses were performed using Excel (Microsoft Office 365) with the add-in software Statcel 4 (OMS Publishing Inc., Japan).

The data were expressed as mean (SD: standard deviation), and differences between groups were considered significant at $P < 0.05$. The data for each group were tested for normality of distribution using the Kolmogorov-Smirnov test. The homogeneity of the groups was confirmed by analyzing the data for each group using Bartlett's test and one-way analysis of variance. The homogeneity of the groups for body weight, extracted muscle weight, room temperature, and humidity were thereby confirmed. The statistical significance of the temperature difference between CSV and CSS was determined using an unpaired *t*-test. Temperature difference between in non-combustion groups was examined by Steel-Dwass test. The protein expression levels were compared using multiple comparison tests, Dunnett's test for soleus muscle and Steel's test for extensor digitorum longus muscle.

III. Results

1. Temperature changes

(1) Pre-measurement—needle body temperature

Figure 1 shows the temperature changes in Pre-measurement for needle body temperature. The temperature of the silver needles at the insertion point increased with each burning, whereas that of the stainless steel needles remained nearly equivalent throughout the three burns. The maximum temperatures of the silver needles for the three burnings were 1st: 64.91 (3.47)°C, 2nd: 68.64 (2.51)°C, 3rd: 70.25 (3.38)°C, and those of the stainless steel needles were 1st: 58.60 (2.06)°C, 2nd: 58.44 (2.80)°C, 3rd: 58.53 (2.66)°C (Fig. 1, Table 1).

The results of the *t*-test for the maximum temperatures of the silver and stainless steel needles were significant at the $P < 0.01$ level for each burning, indicating that the temperature of the needle body of the silver needles increased significantly more than that of the stainless steel needles.

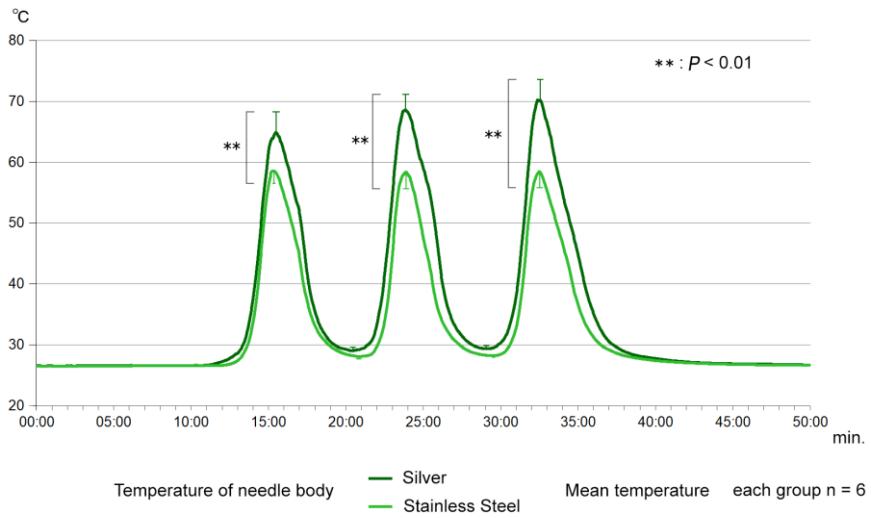

Figure 1. Needle body temperatures in the pre-measurement during three moxa ball burnings

The temperature of the silver and stainless steel needle bodies at the insertion point to the polystyrene foam.

Verticals bars are standard deviation. Asterisks indicate statistical significance between silver and stainless steel (*t*-test).

Table 1.
Pre-measurement: mean (SD) needle body temperature (°C) at the insertion point to the polystyrene foam (each group n = 6)

	At start	Max. at 1st burning	Min. before 2nd burning	Max. at 2nd burning	Min. before 3rd burning	Max. at 3rd burning	Total integral amount
CSV	26.57	64.91 (3.47)	29.04 (0.58)	68.64 (2.51)	29.35 (0.48)	70.25 (3.37)	105,443.44
CSS	26.52	58.60 (2.06)	28.05 (0.41)	58.44 (2.80)	28.22 (2.29)	58.53 (2.66)	97,507.39

Experiment A: mean (SD) skin surface and deep tissue temperatures (°C) at each burning (each group n = 6)
Skin surface temperature

	Min. before 1st burning	Max. at 1st burning	Min. before 2nd burning	Max. at 2nd burning	Min. before 3rd burning	Max. at 3rd burning	Total integral amount
CSV	0.00	8.23 (1.71)	1.97 (0.78)	10.11 (1.80)	2.62 (0.72)	11.25 (1.82)	8494.56
CSS	0.00	7.46 (0.40)	1.58 (0.99)	8.41 (0.57)	1.90 (1.20)	8.36 (0.49)	6622.21

Deep tissue temperature

	Min. before 1st burning	Max. at 1st burning	Min. before 2nd burning	Max. at 2nd burning	Min. before 3rd burning	Max. at 3rd burning	Total integral amount
CSV	0.00	3.09 (0.99)	1.63 (0.67)	4.02 (1.03)	2.19 (0.66)	4.56 (0.92)	4906.03
CSS	0.00	2.32 (1.13)	1.32 (0.85)	2.94 (1.22)	1.63 (0.85)	3.05 (1.21)	3640.69

Experiment B: mean (SD) skin surface temperature (°C) at each burning (each group n = 6)

	Min. before 1st burning	Max. at 1st burning	Min. before 2nd burning	Max. at 2nd burning	Min. before 3rd burning	Max. at 3rd burning	Total integral amount
CSV	0.00	8.16 (1.37)	1.83 (0.64)	10.31 (1.39)	2.32 (0.84)	11.37 (1.31)	8497.15
CSS	0.00	7.18 (0.68)	1.70 (0.52)	8.14 (0.43)	1.96 (0.45)	8.17 (0.86)	6624.14

(2) Experiment A: temperature measurements

As a first step of experiments in rats, we measured the skin surface and deep tissue temperatures simultaneously. Figure 2 shows the time courses of the skin surface and deep tissue temperatures, with the lowest temperature of each group before the first ignition set as the baseline.

The mean maximum skin surface temperatures for the three burnings in CSV were 1st: 8.23 (1.71)°C, 2nd: 10.11 (1.80)°C, and 3rd: 11.25 (1.82)°C. And those in CSS were 1st: 7.46 (0.40)°C, 2nd: 8.41 (0.57)°C, and 3rd: 8.36 (0.49)°C (Fig. 2, Table 1). The results of the *t*-test for the maximum skin surface temperature in the CSV and CSS groups at each burning were significant at the $P < 0.05$ level for the first burning, and at the $P < 0.01$ level for the second and third burnings, indicating that the skin surface temperature increased significantly more in CSV than in CSS.

The mean maximum deep tissue temperatures for the three burnings in CSV were 1st: 3.09 (0.99)°C, 2nd: 4.02 (1.03)°C, and 3rd: 4.56 (0.92)°C, and those in CSS were 1st: 2.32 (1.13)°C, 2nd: 2.94 (1.22)°C, and 3rd: 3.05 (1.21)°C. In the CSV group, both the skin surface and deep tissue temperatures increased stepwise at each burning, and the deep tissue temperature increased and decreased about 2 minutes later than did the skin surface temperature (Fig. 2).

The maximum temperatures at each burning in the CSV group were significantly higher than those in the CSS group (Fig. 2, Table 1). The results of the *t*-test were significant at the $P < 0.05$ level for the first and second burnings, and at the $P < 0.01$ level for the third burning, indicating that the deep tissue temperature increased significantly more in CSV than in CSS.

Figure 3 shows the temperature components in Experiment A. In the CSS group, at the third burning, the deep tissue temperature increased by about 3°C from baseline, and the duration over 3°C was for 65 seconds. In the CSV group, the deep tissue temperature increased by about 4.5°C from baseline at third burning, and the duration over 4.5°C was for 61 seconds (Fig. 3). Throughout the three burnings, temperature increases of over 4°C, over 3.5°C, and over 3°C lasted for 187 seconds, 417 seconds, and 651 seconds, respectively (Fig. 3). The sums of the skin surface temperatures from baseline to the end of the measurements were 8494.56 in CSV and 6622.21 in CSS. For the deep tissue temperature, the same calculation gave 4906.03 in CSV and 3640.69 in CSS (Table 1). In the NSV, NSS, and CON groups, the skin surface and deep tissue temperatures decreased with time (Fig. 5).

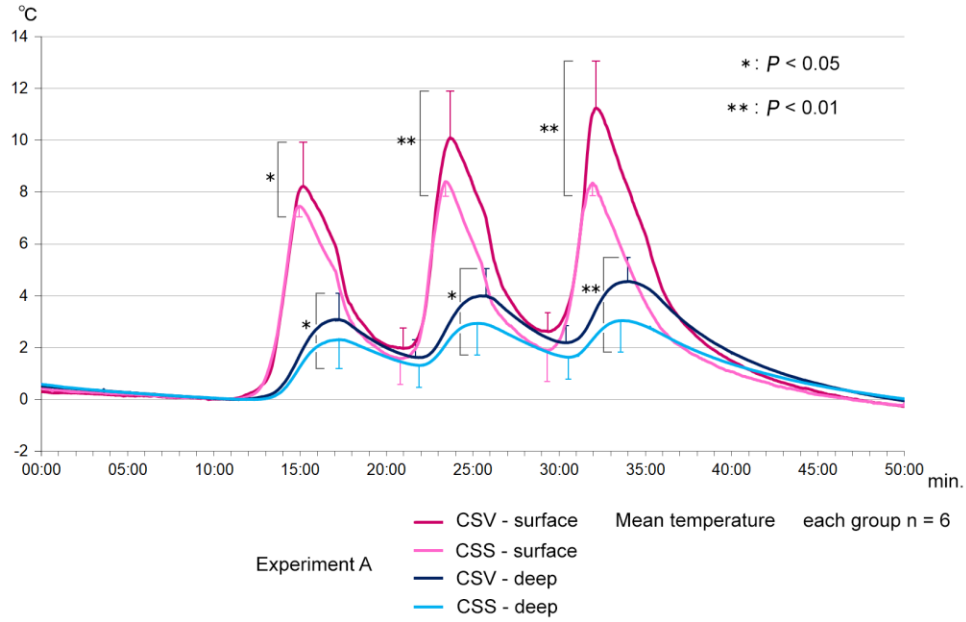

Figure 2. Skin surface and deep tissue temperatures in the combustion groups in Experiment A
CSV: combustion with silver needles, CSS: combustion with stainless steel needles.
Verticals bars are standard deviation. Asterisks indicate statistical significance between CSV and CSS (*t*-test).

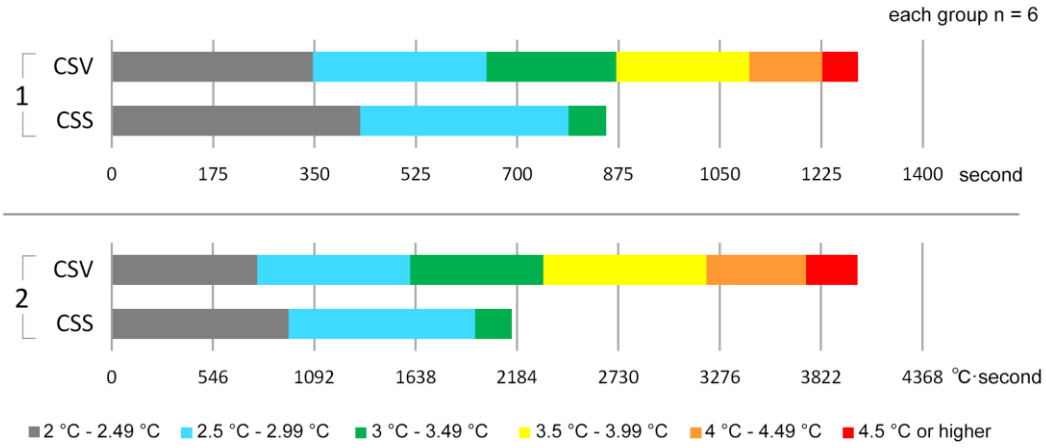

Figure 3. Comparison of high temperature integrals of combustion groups
1: Integral second of each rise in deep tissue temperature
2: Integral amount of each rise in deep tissue temperature
Comparison of high temperature durations and temperature rise integrals in the deep temperatures of the combustion groups in Experiment A. The unit for 1 and 2 is the integrated second and integrated temperature (℃·second), respectively. The unit of ℃·second is adding up the temperature in seconds that was in each of the applicable temperature ranges.
CSV: combustion with silver needles, CSS: combustion with stainless steel needles.
The bars in the 1 and 2 CSVs are the same length, and the graph scales are delimited in the same way.

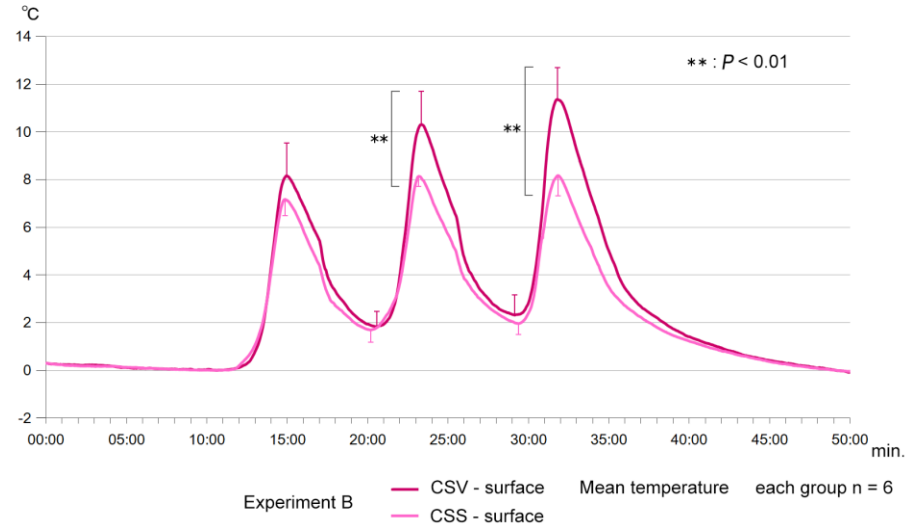

Figure 4. Skin surface temperatures of the combustion groups in Experiment B
CSV: combustion with silver needles, CSS: combustion with stainless steel needles.
Verticals bars are standard deviation. Asterisks indicate statistical significance between CSV and CSS (*t*-test).

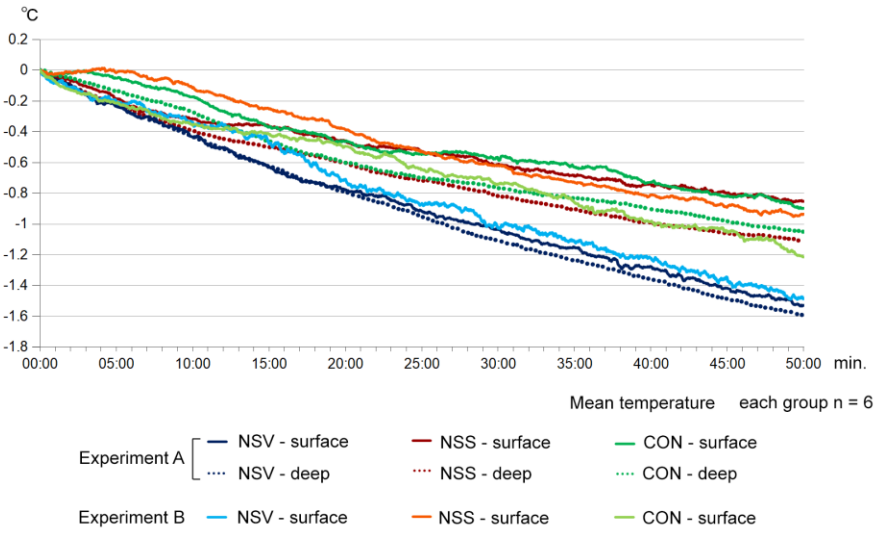

Figure 5. Skin surface and deep temperatures of the non-combustion and control groups in Experiments A and B
NSV: non-combustion with silver needles, NSS: non-combustion with stainless steel needles, CON: control-no needle

(3) Experiment B: αB-crystallin protein expression measurements

As a second step, without inserting a probe to measure the deep tissue temperature, we performed usual moxa needle and measured the skin surface temperature.

Figure 4 shows the time courses of the skin surface temperatures, with the lowest temperature of each group before the first ignition set as the baseline. Skin surface temperatures increased more in CSV than in CSS.

The mean maximum skin surface temperatures in the CSV group for the three burnings were 1st: 8.16 (1.37)°C, 2nd: 10.31 (1.39)°C, and 3rd: 11.37 (1.31)°C, and those in the CSS group were 1st: 7.18 (0.68)°C, 2nd: 8.14 (0.43)°C, and 3rd: 8.17 (0.86)°C.

The maximum temperatures were significantly higher in CSV than in CSS (Fig. 4, Table 1). The results of the *t*-test for the maximum skin surface temperatures in CSV and CSS were significant at the $P < 0.01$ level for the second and third burnings, indicating that the skin surface temperature increased significantly in CSV than in CSS. The sums of the skin surface temperatures from baseline to the end of the measurements were 8497.15 in CSV and 6624.14 in CSS (Table 1). In the NSV, NSS, and CON groups, the skin surface temperatures decreased with time (Fig. 5).

(4) Temperature decreasing in non-combustion groups

The final decreasing temperature data for NSV, NSS, and CON in Experiments A and B were not normally distributed, so the Steel-Dwass test was used to examine whether there were any statistically significant differences among the nine groups; the results showed no significant differences.

2. Expression of alpha B-crystallin

Figure 6 shows the representative blots of αB-crystallin in the soleus of each group and GAPDH as the internal control, and the bar chart of the mean values for each

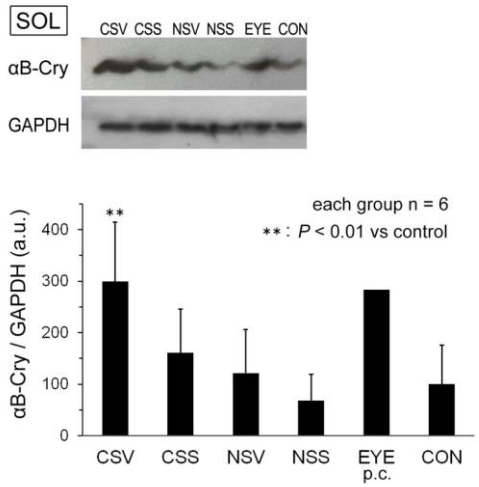

Figure 6. Comparison of αB-crystallin expression in soleus muscle in the control and intervention groups

The levels of αB-crystallin are shown in arbitrary units (a.u.) divided by those of GAPDH, the internal control, and the control group was set as 100. Statistical significance was examined using Dunnett's multiple comparison test.

A representative blot is shown in the upper panel, and the bottom panel shows the relative quantitation.

CSV: combustion with silver needles

CSS: combustion with stainless steel needles

NSV: non-combustion with silver needles

NSS: non-combustion with stainless steel needles

EYE p.c.: positive control

CON: control-no needle

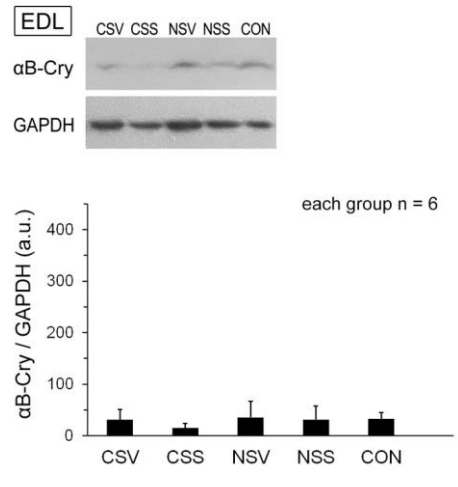

Figure 7. Comparison of αB-crystallin expression in the extensor digitorum longus muscle in the control and intervention groups

The levels of αB-crystallin are shown in arbitrary units (a.u.) divided by those of GAPDH, the internal control, as the ratio of soleus control group set as 100. Statistical significance was examined using Steel's multiple comparison test.

A representative blot is shown in the upper panel, and the bottom panel shows the relative quantitation.

CSV: combustion with silver needles

CSS: combustion with stainless steel needles

NSV: non-combustion with silver needles

NSS: non-combustion with stainless steel needles

CON: control-no needle

group. Regarding αB-crystallin expression in the soleus of the stimulated side after correction for GAPDH expression, when the CON group was set at 100 (75.23), CSV was 299.29 (115.57), CSS was 160.62 (85.39), NSV was 121.51 (84.11), NSS was 67.52 (51.19), and eyeballs as the positive control was 283.25. Statistical significance was examined using Dunnett's multiple comparison test.

The results revealed a significant difference between the CON and CSV groups, with the CSV group showing significantly higher expression of αB-crystallin than the CON group ($P < 0.01$).

Figure 7 shows the representative blots of αB-crystallin in the EDL of each group and GAPDH as the internal control, and the bar chart of the mean values of each group. Regarding αB-crystallin expression in the EDL of the stimulated side after correction for GAPDH expression, when CON of soleus was set at 100, CSV was 30.73 (20.03), CSS was 14.33 (9.62), NSV was 35.12 (31.21), NSS was 31.05 (26.42), and CON was 32.16 (12.90). As the data did not follow a normal distribution, Steel's test was used for multiple comparisons, and the results showed no significant differences among the intervention and control groups.

IV. Discussion

1. Relationship between the temperature increase required for chaperone activity and temperature changes with different needle materials

The fact that the courses of the skin surface temperature change in Experiments A and B were almost similar suggests that the course of the deep tissue temperature in Experiment B was almost similar to the course of Experiment A. Therefore, in Experiment B, it must be the deep tissue temperature of the moxa needle combustion group increased approximately 4.5°C with silver needles and approximately 3°C with stainless steel needles. It is speculated that this difference in temperature increase caused a difference in the effects on the expression of molecular chaperones.

Many previous studies have examined the temperature setting for thermal stimulation of the skin surface, but not those for deep tissue [14–18]. We consider that heat shock protein expression in skeletal muscles should be examined in relation to deep tissue temperature changes.

From the results of this study, it can be inferred that a deep tissue temperature increase from 4°C to 5°C for about 3 minutes is required to increase αB-crystallin expression. In CSS group, the duration of temperature differences of over 3°C was short, so it is assumed that such a brief and weak stimulation would have little or no effect on the increase in heat shock proteins.

On the other hand, in the CSV group, the deep tissue temperature increased by about 4.5°C at the third burning, and the duration over 3°C was 10 times longer than that in the CSS group (Fig.3). As it is fairly certain that the radiant heat from the combustion of moxa balls was almost similar for both CSV and CSS, the fact that both skin surface and deep tissue temperatures were significantly higher in CSV than in CSS can be attributed to differences in the heat conduction of the needles.

During a local temperature increase, heat diffusion by blood flow is considered to occur, and unless the heat supply exceeds that rate, the temperature will not rise above a certain level. Therefore, it is considered that in CSV with a large heat supply, the temperature increased stepwise with each burning, and in CSS with not a large heat supply, the temperature increased similarly to the second and third burnings.

A comparison of the duration of the deep tissue temperature rise and the integral amount of temperature revealed that the difference between the CSV and CSS groups was greater for the integral amount of temperature rise than for the duration (Fig. 3), which indicated that the degree of increase during the period of the temperature rise was smaller in CSS than in CSV, and thus, the rate of deep tissue temperature change was faster in CSV than in CSS.

Our results revealed that moxa needle with silver needles could rapidly raise the local deep tissue temperature. The rate of temperature change affects the sensory warm and cold thresholds, with slower temperature changes thresholds increase steadily[20]. As the rate of temperature change affects sensory perception, it may also affect chaperone expression. Sciatic denervation also affects chaperone expression in the lower extremities[18,21], suggesting involvement of the central nervous system. Moreover, the rate of temperature change ascending the sensory pathways may also be a stressor. However, we recognize that this supposition requires an examination of the rate of temperature change between CSV and CSS.

2. Characteristics of moxa needle thermal stimulation

Thermal stimulation using moxa needle, unlike stimulation such as prolonged immersion in hot water or other thermotherapies, is localized, with a short duration of high temperature and a small stimulation area, so there is no risk of heat stroke.

It has not been clear how the specific thermal stimulation of moxa needles acts as a stressor and leads to the expression of heat shock proteins. The time course in CSV that moxa needle with silver needles showed, not only increases in the skin surface and deep tissue temperature but also a considerable decrease in temperature after the internal combustion of the moxa ball is over.

Although the difference was not statistically significant, in the NSV, NSS, and CON groups, both the surface and deep tissue temperatures showed a slightly downward trend in the NSV with silver needles compared with NSS and CON (Fig. 5). The reason for this may be that some body heat was lost due to conduction by the silver needle. In the same way, the temperature decrease after combustion in CSV was likely due to the high thermal conductivity of silver, which allows heat to escape

through the needles. When this increase and decrease were repeated, it was presumed that the greater the fluctuation, the greater the stressor, and the greater the increase of αB-crystallin expression.

Moxa needle stimulation does not apply the same amount of heat to all surfaces, unlike stimulation such as immersion in warm water, and the temperature increase varies with the depth of the muscle, so comparisons cannot be made under the same conditions. Therefore, the EDL values in this study are reference data. It is known that the expression of αB-crystallin is low under thermal stimulation in EDL, a fast-twitch muscle[17,18]. In the present study, αB-crystallin expression was lower in the EDL than in the soleus muscle, and no stimulus-induced changes were observed. It is thought that the entire rat lower leg was elevated by the combustion of a moxa ball approximately 2 cm in diameter. However, moxa needle was applied to the posterior surface of the lower leg, even if the needle tip is right next to the fibula and in the vicinity of EDL, the temperature rise in the anterior muscles of the lower leg was considered to be smaller than that in the posterior ones.

3. Effects and usefulness of moxa needle with silver needles in soleus

The results of this study clarified that moxa needle with silver needles compared to the stainless steel needles influence the generation of molecular chaperones by increasing the temperature not only on the skin surface, but also in the deep tissue. It is assumed that the effects of moxa needle with silver needles differ from those of stainless steel needles, which have thermal stimulation by mainly radiant heat in addition to mechanical stimulation by the insertion of the needle.

It has been reported that heat stress increases Hsp72 expression in soleus, plantaris, and EDL muscles, among which, muscle mass gain occurs only in the soleus, which is a slow antigravity muscle[19]; this suggests that it is not Hsp72 that is responsible for the muscle mass gain. Alpha B-crystallin is specific to slow-twitch muscle fibers and increases by thermal stimulation, as shown in previous studies[22] and also suggested in the present study, and thus may be functional for the increase in the mass of soleus muscles which contains many slow-twitch muscle fibers[23].

Heat therapy is a very promising area of physiology research, as it has the potential to contribute to approaches addressing disuse atrophy in aging adults or those under microgravity circumstances. The idea of using metal heat conduction to raise the deep tissue temperature may provide an opportunity to explore factors contributing to the development of not only moxa needle but also further new methods. It is suggested that a new position may be established as an effect of traditional moxa needle, and a new aspect may be added to the purpose of moxa needle therapy. The present results showed an increase in αB-crystallin, which is required for the maintenance of slow-twitch muscle fibers, and so we will continue our research in order to contribute to the prevention of muscle atrophy and the strengthening of standing posture retention.

V. Conclusions

The results of this study suggest that a deep tissue temperature increase from 4°C to 5°C for about 3 minutes is required to increase αB-crystallin expression. Therefore, in moxa needle stimulation to the posterior surface of the lower leg, the use of silver needles with high thermal conductivity could increase the deep tissue temperature and expression of αB-crystallin in soleus muscles.

Acknowledgments

We are grateful to Dr. Yoshihisa Naruse (Tokoha University) and Mr. Yoshiyuki Okamoto (Meiji School of Oriental Medicine) for their excellent technical support of this study, and also grateful to Dr. Manami Itoi and Dr. Satomi Ebara (Meiji University of Integrative Medicine) for their encouragement and continuous support.

Conflict of interest

There is no conflict of interest in this study.

The pre-study for this paper was presented at the annual congress of the Japan Society of Acupuncture and Moxibustion in Tokyo (71th, 2022). The contents of this paper have not previously been published in any language and are not under consideration by another journal.

References

1) Ellis J. Proteins as molecular chaperones. Nature. 1987; 328: 378–9.
2) Basha E, O'Neill H, Vierling E. Small heat shock proteins and α-crystallins: dynamic proteins with flexible functions. Trends Biochem Sci. 2012; 37(3): 106–17.
3) Horwitz J. Alpha-crystallin can function as a molecular chaperone. Proceedings of the National Academy of Sciences of the United States of America. 1992; 89: 10449–53.
4) Dubin R, Wawrousekt E, Piatigorsky J. Expression of the Murine αB-Crystallin Gene is not restricted to the Lens. Mol Cell Biol. 1989; 9(3): 1083–91.
5) Ohto-Fujita E, Hayasaki S, Atomi A, Fujiki S, Watanabe T, Boelens W, et al. Dynamic localization of αB-crystallin at the microtubule cytoskeleton network in beating heart cells. The Journal of Biochemistry. 2020; 168(2): 125–37.
6) Sakurai T, Fujita Y, Ohto E, Oguro A, Atomi Y. The decrease of the cytoskeleton tubulin follows the decrease of the associating molecular chaperone αB-crystallin in unloaded soleus muscle atrophy without stretch. FASEB J. 2005; 19(9): 1199–201.
7) Atomi Y, Yamada S, Hong Y. Dynamic Expression of αB-crystallin in Skeletal Muscle, Effects of

Unweighting, Passive Stretch and Denervation. Proc Jpn Acad Ser B. 1990; 66(10): 203–8.
8) Atomi Y, Yamada S, Strohman R, Nonomura Y. Alpha B-crystallin in skeletal muscle: purification and localization. J Biochem. 1991; 110(5): 812–22.
9) D'Amico D, Fiore R, Caporossi D, Felice V, Cappello F, Dimauro I, et al. Function and Fiber-Type Specific Distribution of Hsp60 and αB-Crystallin in Skeletal Muscles: Role of Physical Exercise. Biology. 2021; 10(2): 77.
10) Arai H, Atomi Y. Chaperone activity of alpha B-crystallin suppresses tubulin aggregation through complex formation. Cell Struct Funct. 1997; 22(5): 539–44.
11) Akabane K. Methods of Moxa Needle (Kyutoshinhou). IDO-NO-NIPPON SHA INC. 1971. (in Japanese)
12) Tanaka H. Moxa Needle—Instruction and Guidance of the Therapy (Kyutoshin Nyumon). Orient Publisher. 1991. (in Japanese)
13) Yajima M, Tanaka H. Moxa Needle Therapy. In: Kitade T, Shinohara S (eds.). A Guide to Special Acupuncture Techniques—The Practical and Clinical Application (Tokushu Shinkyu Tekisuto). Ishiyaku Publishers,Inc. 2014; 129–34. (in Japanese)
14) Kim K, Reid B, Casey C, Bender B, Ro B, Song Q, et al. Effects of repeated local heat therapy on skeletal muscle structure and function in humans. J Appl Physiol. 2020; 128(3): 483–92.
15) Naito H, Powers S, Demirel H, Sugiura T, Dodd S, Aoki J. Heat stress attenuates skeletal muscle atrophy in hindlimb-unweighted rats. J Appl Physiol. 2000; 88(1): 359–63.
16) Yoshida N, Morimoto Y, Kataoka H. Effects of Combination Therapy of Heat Stress and Muscle Contraction Exercise Induced by Neuromuscular Electrical Stimulation on Disuse Atrophy in the Rat Gastrocnemius. J. Phys. Ther. Sci. 2013; 25(2): 201–6.
17) Lee J, Abe M, Tatebayashi D, Himori K, Yamada T. Effect of intermittent heat stress on contractile function in extensor digitorum longus muscle from adjuvant-induced arthritis rats. Japanese journal of physical therapy fundamentals. 2016; 19(2): 39–47. (in Japanese)
18) Abe M, Lee J, Tsuchiyama M, Yamada T. Effects of heat stress on contractile properties in denervated rat skeletal muscle. Japanese journal of physical therapy fundamentals. 2013; 17(1): 53–62. (in Japanese)
19) Kobayashi T, Uehara K, Goto K, Kojima A, Honda M, Akema T, et al. Muscular hypertrophy is induced by heat stress in rat skeletal muscles. The St. Marianna Medical Journal. 2003; 31: 131–8. (in Japanese)
20) Schmidt R. Fundamentals of Sensory Physiology. Second, Corrected Edition (English Edition), New York, Springer-Verlag. 1981; 102–10.
21) Inaguma Y, Goto S, Shinohara H, Hasegawa K, Ohshima K, Kato K. Physiological and Pathological Changes in Levels of the Two Small Stress Proteins, HSP27 and αB Crystallin, in Rat Hindlimb Muscles. J Biochem. 1993; 114(3): 378–84.
22) Larkins NT, Murphy RM, Lamb GD. Absolute amounts and diffusibility of HSP72, HSP25, and αB-crystallin in fast- and slow-twitch skeletal muscle fibers of rat. Am J Physiol Cell Physiol. 2012; 302(1): C228–39.
23) Soukup T, Zachařová G, Smerdu V. Fibre type composition of soleus and extensor digitorum longus muscles in normal female inbred Lewis rats. Acta Histochem. 2002; 104(4): 399–405.